

1 Dynamics of Spike-Specific Neutralizing Antibodies Across Five-Year Emerging SARS-CoV-2
2 Variants of Concern Reveal Conserved Epitopes that Protect Against Severe COVID-19

3
4 Latifa Zayou^{1, 2 #}; Swayam Prakash^{1, #}; Hawa Vahed⁶; Nisha Rajeswari Dhanushkodi^{1*}; Afshana
5 Quadiri^{1*}; Ahmed Belmouden²; Zohra Lemkhente³; Aziz Chentoufi¹; Daniel Gil⁶, Jeffrey B. Ulmer⁶ &
6 Lbachir BenMohamed^{1, 4, 5, 6 †}

7
8 ¹Laboratory of Cellular and Molecular Immunology, Gavin Herbert Eye Institute, University of California
9 Irvine, School of Medicine, Irvine, CA 92697; ²Laboratory of Cell Biology and Molecular Genetics,
10 Faculty of Sciences, Ibn Zohr University, Agadir, Morocco; ³Laboratory of Medical-Surgical,
11 Biomedicine and infectiology Research, Faculty of Medicine and Pharmacy, Ibnou Zohr University,
12 Agadir, Morocco; ⁴Department of Molecular Biology and Biochemistry; ⁵Institute for Immunology; the
13 University of California Irvine, School of Medicine, Irvine, CA 92697, ⁶Department of Vaccines and
14 Immunotherapies, TechImmune, LLC, University Lab Partners, Irvine, CA 92660; USA

15
16 Running Title: Cross-Protective Conserved B cell epitopes

17
18 #Authors have contributed equally to this study

19 Corresponding Author: Professor Lbachir BenMohamed, Laboratory of Cellular and Molecular
20 Immunology, Gavin Herbert Eye Institute, the University of California Irvine, School of Medicine, Hewitt
21 Hall, Room 2032; 843 Health Sciences Rd.; Irvine, CA 92697-4390; Phone: 949-824-8937. Fax: 949-
22 824-9626. E-mail: Lbenmoha@uci.edu.

23 Conflict of interest: Studies of this report were supported by Public Health Service Research grants
24 AI158060, AI150091, AI143348, AI147499, AI143326, AI138764, AI124911, and AI110902 from the
25 National Institutes of Allergy and Infectious Diseases (NIAID) to LBM and by R43AI174383 to
26 TechImmune, LLC. LBM has an equity interest in TechImmune, LLC., a company that may potentially
27 benefit from the research results and serves on the company's Scientific Advisory Board. LBM's
28 relationship with TechImmune, LLC., has been reviewed and approved by the University of California,
29 Irvine in accordance with its conflict-of-interest policies.

30
31 Keywords: SARS-CoV-2; COVID-19; B cell epitopes; Antibodies; Age; Gender; Disease Severity.

32

33

ABSTRACT

34

35 Since early 2020, several SARS-CoV-2 variants of concern (VOCs) continue to emerge, evading
36 waning antibody mediated immunity produced by the current Spike-alone based COVID-19 vaccines.
37 This caused a prolonged and persistent COVID-19 pandemic that is going to enter its fifth year. Thus,
38 the need remains for innovative next generation vaccines that would incorporate protective Spike-
39 derived B-cell epitopes that resist immune evasion. Towards that goal, in this study we (i) Screened the
40 sequences of Spike among many VOCs and identified conserved and non-conserved linear B-cell
41 epitopes; (ii) Compared titers and neutralization antibodies specific to these conserved and non-
42 conserved B-cell epitopes from serum of symptomatic and asymptomatic COVID-19 patients that were
43 exposed to multiple VOCs across the 5-year COVID-19 pandemic, and (iii) Compared protective efficacy
44 of conserved versus non-conserved B-cell epitopes against the most pathogenic Delta variant in a
45 “humanized” ACE-2/HLA transgenic mouse model. We found robust conserved B-cell epitope-specific
46 antibody titers and neutralization in sera from asymptomatic COVID-19 patients. In contrast, sera from
47 symptomatic patients contained weaker antibody responses specific to conserved B-cell epitopes. A
48 multi-epitope COVID-19 vaccine that incorporated the conserved B-cell epitopes, but not the non-
49 conserved B-cell epitopes, significantly protected the ACE2/HLA transgenic mice against infection and
50 COVID-19 like symptoms caused by the Delta variant. These findings underscore the importance of
51 conserved B-cell epitopes in generating robust protective immunity against severe COVID-19
52 symptoms caused by various VOCs, providing valuable insights for the development of broad-spectrum
53 next generation Coronavirus vaccines capable of conferring cross-variant protective immunity.

54

55

56

57
58
59
60
61
62
63
64
65
66
67
68
69
70
71
72
73
74
75
76
77
78

IMPORTANCE

A persistent COVID-19 pandemic continues to evolve because of a continued emergence of SARS-CoV-2 variants of concern (VOCs) that escape the antibodies induced by the current Spike-alone COVID-19 vaccines. Identifying and characterizing the protective and non-protective Spike-derived B-cell epitopes that resist immune-evasion is a paramount for the development of broad-spectrum next generation Coronavirus vaccines. The present study identified Spike-derived conserved B cell epitopes that (i) are targeted by consistent and strong antibody responses in asymptomatic COVID-19 patients across the 5-year pandemic regardless of VOCs; and (ii) provided strong protection in ‘humanized’ ACE2/HLA transgenic mice against infection and COVID-19 like symptoms caused by the most pathogenic Delta variant. The findings have the potential to inform the design of next generation Coronavirus vaccines capable of conferring cross-variant protective immunity.

79

TWEET

80 Protective SARS-CoV-2 Conserved Linear B Cell Epitopes Identified from Spike Protein.

81

INTRODUCTION

82

83 Since early 2020, the world has encountered successive waves of COVID-19, fueled by the
84 emergence of over 20 variants of concern (VOCs) with maintained transmissibility and virulence (4). As
85 of September 2024, the number of confirmed SARS-CoV-2 cases has reached over 776 million, and
86 COVID-19 has caused over 7 million deaths (1-3). The world will enter its sixth year of a persistent
87 COVID-19 pandemic, fueled by the continuous emergence of heavily Spike-mutated and highly
88 contagious SARS-CoV-2 variants and sub-variants that continue to: (i) escaped immunity induced by
89 the current Spike-alone-based vaccines; (ii) disrupt the efficacy of the COVID-19 booster paradigm (5-
90 10); and (iii) outpace the development of variant-adapted bivalent Spike-alone vaccines (1-3, 11, 12).
91 This bleak outlook of a prolonged COVID-19 pandemic emphasizes the urgent need for developing a
92 next-generation broad-spectrum pan-Coronavirus vaccine capable of conferring strong cross-variant and
93 cross-strain protective immunity that would prevent immune evasion and breakthrough infections (12).

94 The Spike protein is heavily mutated in these variants with an accumulated 346 mutations since
95 the ancestral Wuhan strain, including 60 and 52 new mutations, in BA.2.86 and JN.1 Omicron
96 subvariants, respectively. As such the Omicron variant exhibits reduced susceptibility to vaccine-
97 induced neutralizing antibodies, requiring a boost to generate protective immunity (13). The dynamics
98 of SARS-CoV-2 virus neutralization are integral to understanding and enhancing the efficacy of COVID-
99 19 vaccines. Understanding the dynamics of Spike neutralizing antibodies would inform vaccine booster
100 strategies and help to predict the impact of new variants on vaccine-induced immunity. The changing
101 dynamics of SARS-CoV-2 virus neutralization plays a crucial role in determining the efficacy of COVID-
102 19 vaccines and it depends on (i) the level of Neutralizing Antibody production, (ii) the role of emerging
103 SARS-Cov-2 variants of concerns (VOCs), (iii) the role of immune escape mechanisms by emerging
104 SARS-CoV-2 variants, and (iv) booster doses of COVID-19 vaccines. We previously, mapped and
105 characterized the antigenicity and immunogenicity of genome-wide linear B cell epitopes that are highly
106 conserved (1). We demonstrated that conserved B cell epitopes provided cross-protection against all

107 the emerging SARS-CoV-2 variants of concern (VOCs), i.e., Alpha (B.1.1.7), Beta (B.1.351), Gamma
108 (P.1), Epsilon (B.1.427/B.1.429), Delta (B.1.617.2), and Omicron (B.1.1.529) in a north American
109 COVID-19 population cohort. In the present study, we hypothesize that multi-epitope vaccine
110 candidates that incorporate highly conserved, antigenic, and immunogenic B cell epitopes will provide
111 broader protection against COVID-19 caused by multiple SARS-CoV-2 VOCs.

112 We identified six B cell epitopes that are highly conserved within all the 20 VOCs of SARS-CoV-
113 2, SARS-CoV, MERS-CoV, common cold Coronaviruses (HKU, OC1, 229E, NL63), and animal CoVs
114 strains (i.e., Bats, Civet Cats, Pangolin and Camels). We established that those epitopes were
115 selectively recognized by antibodies from “naturally protected” asymptomatic COVID-19 patients. In
116 contrast symptomatic patients exhibited weaker antibody titers specific to conserved B-cell epitopes.
117 Accordingly, antibodies from asymptomatic COVID-19 patients, but not from symptomatic patients,
118 exhibited higher neutralization efficacy. Immunization of ACE2/HLA transgenic mice with a mixture of
119 conserved B-cell epitopes significantly protected against infection and COVID-19 like symptoms caused
120 by Delta variant. This study underscores the importance of conserved B-cell epitopes in generating
121 robust protective immunity against severe disease caused by various SARS-CoV-2 variants, providing
122 valuable insights for the development of broad-spectrum vaccines against COVID-19.

123

124

125

126

127

128

129

130

131

132

MATERIALS & METHODS

133

134

135

136

137

138

139

140

141

142

143

144

145

146

147

148

149

150

151

152

153

154

155

156

157

Human study population cohort and HLA genotyping: We enrolled 210 subjects from a pool of over 682 subjects. Written informed consent was obtained from participants before inclusion. The subjects were categorized as mild to severe COVID-19 groups and have undergone treatment at the University of California Irvine Medical Center between July 2020 to July 2022 (Institutional Review Board protocol # 2020-5779). SARS-CoV-2 positivity was defined by a positive RT-PCR on nasopharyngeal swab samples. All the subjects were genotyped by PCR for class I HLA-A*02:01 and class II HLA-DRB1*01:01 among the 682 patients (and after excluding a few for which the given amount of blood was insufficient - i.e., less than 6ml), ending with 210 that were genotyped for HLA-A*02:01⁺ or/and HLA-DRB1*01:01⁺ (15, 16). Based on the severity of symptoms and ICU admission/intubation status, the subjects were divided into two broad severity categories namely: Symptomatic (patients who died from COVID-19 complications, infected COVID-19 patients with severe disease that were admitted to the intensive care unit (ICU) and required ventilation support, infected COVID-19 patients with severe disease that required enrollment in ICU but without ventilation support, infected COVID-19 patients with moderate symptoms that involved a regular hospital admission or infected COVID-19 patients with mild symptoms) and Asymptomatic (infected individuals with no symptoms).

Sequence comparison among variants of SARS-CoV-2 and animal CoV strains: We retrieved nearly 8.5 million human SARS-CoV-2 genome sequences from the GISAID database representing countries from North America, South America, Central America, Europe, Asia, Oceania, Australia, and Africa. All the sequences included in this study were retrieved either from the NCBI GenBank (www.ncbi.nlm.nih.gov/nucleotide) or GISAID (www.gisaid.org). Multiple sequence alignment was performed keeping SARS-CoV-2-Wuhan-Hu-1 (MN908947.3) protein sequence as a reference against all the SARS-CoV-2 VOCs, common cold, and animal CoV strains. The sequences were aligned using the high throughput alignment tool DIAMOND (17). This comprised of all the VOCs and VBMs of SARS-CoV-2 (B.1.177, B.1.160, B.1.1.7, B.1.351, P.1, B.1.427/B.1.429, B.1.258, B.1.221, B.1.367,

158 B.1.1.277, B.1.1.302, B.1.525, B.1.526, S:677H.Robin1, S:677P.Pelican, B.1.617.1, B.1.617.2,
159 B,1,1,529) and common cold SARS-CoV strains (SARS-CoV-2-Wuhan-Hu-1 (MN908947.3), SARS-
160 CoV-Urbani (AY278741.1), HKU1-Genotype B (AY884001), CoV-OC43 (KF923903), CoV-NL63
161 (NC_005831), CoV-229E (KY983587)) and MERS (NC_019843)). We have included whole-genome
162 sequences from the bat ((RATG13 (MN996532.2), ZXC21 (MG772934.1), YN01 (EPI_ISL_412976),
163 YN02(EPI_ISL_412977), WIV16 (KT444582.1), WIV1 (KF367457.1), YNLF_31C (KP886808.1), Rs672
164 (FJ588686.1)), pangolin (GX-P2V (MT072864.1), GX-P5E (MT040336.1), GX-P5L (MT040335.1), GX-
165 P1E (MT040334.1), GX-P4L (MT040333.1), GX-P3B (MT072865.1), MP789 (MT121216.1),
166 Guangdong-P2S (EPI_ISL_410544)), camel (KT368891.1, MN514967.1, KF917527.1, NC_028752.1),
167 and civet (Civet007, A022, B039)) in evaluating the evolutionary relationship among the SARS-CoV-2
168 variants and common cold CoV strains,

169 **Data and Code Availability:** The human-specific SARS-CoV-2 complete genome sequences
170 were retrieved from the GISAID database, whereas the SARS-CoV-2 sequences for pangolin (*Manis*
171 *javanica*), and bat (*Rhinolophus affinis*, *Rhinolophus malayanus*) were retrieved from NCBI. Genome
172 sequences of previous strains of SARS-CoV for humans, bats, civet cats, and camels were retrieved
173 from the NCBI GenBank.

174 **SARS-CoV-2 B Cell Epitope Prediction:** Linear B cell epitope predictions were carried out on
175 the spike glycoprotein (S), the primary target of B cell immune responses for SARS-CoV. We used the
176 BepiPred 2.0 algorithm embedded in the B cell prediction analysis tool hosted on the IEDB platform.
177 For each protein, the epitope probability score for each amino acid and the probability of exposure was
178 retrieved. Potential B cell epitopes were predicted using a cutoff of 0.55 (corresponding to a specificity
179 greater than 0.81 and sensitivity below 0.3) and considering sequences having more than 5 amino acid
180 residues. This screening process resulted in 8 B-cell peptides. These epitopes represent all the major
181 non-synonymous mutations reported among the SARS-CoV-2 variants. One B-cell epitope (S₄₃₉₋₄₈₂)
182 was observed to possess the maximum number of variant-specific mutations. Structure-based antibody
183 prediction was performed using Discotope 2.0, and a positivity cutoff greater than -2.5 was applied

184 (corresponding to specificity greater than or equal to 0.80 and sensitivity below 0.39), using the SARS-
185 CoV-2 spike glycoprotein structure (PDB ID: 6M1D).

186 **Protein-peptide molecular docking:** Computational peptide docking of B cell peptides into the
187 ACE2 complex (binding protein) was performed using the GalaxyPepDock under GalaxyWEB. To
188 retrieve the ACE2 structure, we used the x-ray crystallographic structure ACE2-B0AT1 complex 6M1D
189 available on the Protein Data Bank. The 6M1D with a structural weight of 334.09 kDa possesses two
190 unique protein chains, 2,706 residues, and 21,776 atoms. In this study, flexible target docking based
191 on an energy-optimization algorithm was carried out on the ligand-binding domain containing ACE2
192 within the 4GBX structure. Similarity scores were calculated for protein-peptide interaction pairs for each
193 residue. The prediction accuracy is estimated from a linear model as the relationship between the
194 fraction of correctly predicted binding site residues and the template-target similarity measured by the
195 protein structure similarity score and interaction similarity (S_{Inter}) score obtained by linear regression.
196 S_{Inter} shows the similarity of amino acids of the B cell peptides aligned to the contacting residues in the
197 amino acids of the ACE2 template structure. Higher S_{Inter} score represents a more significant binding
198 affinity among the ACE2 molecule and B cell peptides. Subsequently, molecular docking models were
199 built based on distance restraints for protein peptide pairs using GalaxyPepDock. Based on the
200 optimized energy scores, docking models were ranked.

201 **Peptide synthesis:** Potential B cell epitopes identified from human-SARS-CoV-2 spike protein,
202 were synthesized using solid-phase peptide synthesis and standard 9-fluorenylmethoxycarbonyl
203 technology (21st Century Biochemicals, Marlborough, MA). The purity of peptides was over 90%, as
204 determined by reversed-phase HPLC (Vydac C18) and mass spectroscopy (Voyager MALDI-TOF
205 System). Stock solutions were made at 1 mg/ml in 10% DMSO in PBS.

206 **TaqMan quantitative polymerase reaction assay for the screening of SARS-CoV-2**
207 **Variants in COVID-19 patients:** We utilized a laboratory-developed modification of the CDC SARS-
208 CoV-2 RT-PCR assay, which received Emergency Use Authorization by the FDA on April 17th, 2020.
209 (<https://www.fda.gov/media/137424/download> [accessed 24 March 2021]).

210 **Mutation screening assays:** SARS-CoV-2-positive samples were screened by four
211 multiplex RT-PCR assays. Through the qRT-PCR, we screened for 11 variants of SARS-CoV-2 in
212 our patient cohort. The variants which were screened include B.1.1.7 (Alpha), B.1.351 (Beta), P.1
213 (Gamma), and B.1.427/B.1.429 (Epsilon), B.1.525 (Eta), R.1, P.2 (Zeta), B.1.526 (Iota),
214 B.1.2/501Y or B.1.1.165, B.1.1.529 (BA.1) (Omicron), B.1.1.529 (BA.2) (Omicron), and B.1.617.2
215 (Delta). The sequences for the detection of $\Delta 69-70$ were adapted from a multiplex real-time RT-
216 PCR assay for the detection of SARS-CoV-2 (18). The probe overlaps with the sequences that
217 contain amino acids 69 to 70; therefore, a negative result for this assay predicts the presence of
218 deletion S- $\Delta 69-70$ in the sample. Using a similar strategy, a primer/probe set that targets the
219 deletion S- $\Delta 242-244$ was designed and was run in the same reaction with S- $\Delta 69-70$. In addition,
220 three separate assays were designed to detect spike mutations S-501Y, S-484K, and S-452R and
221 wild-type positions S-501N, S-484E, and S-452L.

222 Briefly, 5 μ l of the total nucleic acid eluate was added to a 20 μ l total-volume reaction
223 mixture (1x TaqPath 1-Step RT-qPCR Master Mix, CG [Thermo Fisher Scientific, Waltham, MA], with
224 0.9 mM each primer and 0.2 mM each probe). The RT-PCR was carried out using the ABI
225 StepOnePlus thermocycler (Life Technologies, Grand Island, NY). The S-N501Y, S-E484K, and S-
226 L452R assays were carried out under the following conditions: 25°C for 2 min, then 50°C for 15 min,
227 followed by 10 min at 95°C and 45 cycles of 95°C for 15 s and 65°C for 1 min. The $\Delta 69-70$ / $\Delta 242-$
228 244 assays were run under the following conditions: 25°C for 2 min, then 50°C for 15 min, followed
229 by 10 min at 95°C and 45 cycles of 95°C for 15 s and 60°C for 1 min. Samples displaying typical
230 amplification curves above the threshold were considered positive. Samples that yielded a negative
231 result or results in the S- $\Delta 69-70/\Delta 242-244$ assays or were positive for S-501Y P2, S-484K P2, and S-
232 452R P2 were considered screen positive and assigned to a VOC.

233 **Enzyme-linked immunosorbent assay (ELISA):** Serum antibodies specific for epitope
234 peptides and SARS-CoV-2 proteins were detected by ELISA. 96-well plates (Dynex Technologies,
235 Chantilly, VA) were coated with 0.5 μ g peptides or 100 ng S protein per well at 4°C overnight,

236 respectively, and then washed three times with PBS and blocked with 3% BSA (in 1 X PBS) for 2hours.
237 at RT. After blocking, the plates were incubated with 1:200 dilutions of the sera (100 µl/well) overnight
238 at 4°C. The bound serum antibodies were detected with HRP-conjugated goat anti-mouse IgG and
239 chromogenic substrate TMB (ThermoFisher, Waltham, MA). The cut-off for seropositivity was set as the
240 mean value plus three standard deviations (3SD) in HBc-S control sera. The binding of the epitopes to
241 the sera of SARS-CoV-2 infected samples was detected by ELISA using the same procedure, 96-well
242 plates were coated with 0.5 µg peptides and sera were diluted at 1:50. All ELISA studies were performed
243 at least twice.

244 **Neutralizing antibody assays for SARS-CoV-2:** Serially diluted heat-inactivated plasma (1:3)
245 and 300 PFU of SARS-CoV-2 variants were combined in Dulbecco's Modified Eagle's Medium (DMEM)
246 and incubated at 37°C 5% CO₂ for 30 minutes. After neutralization, the antibody-virus inoculum was
247 transferred onto Vero E6 cells (ATCC C1008) and incubated at 34°C 5% CO₂ for 1 hour. The cells
248 were then fixed with 10% neutral buffered formalin and incubated at -20°C for 10 minutes followed by
249 20 minutes at room temperature. Plates were developed with True Blue HRP substrate and imaged
250 on an ELISpot reader. The half maximum inhibitory concentration (IC₅₀) was calculated using
251 normalized counted foci.

252 **Triple transgenic mice immunization with multi-epitope Pan-Coronavirus vaccine and**
253 **infection:** The animal studies were performed at the University of California Irvine and adhered to
254 the Guide for the Care and Use of Laboratory Animals published by the US National Institute of Health.
255 All animal experiments were performed under the approved IACUC protocol # AUP-22-086. Female
256 HLA-DR*0101/HLA-A*0201/hACE2 triple transgenic mice (8-9 weeks old) were used in this study.
257 The HLA-DR*0101/HLA-A*0201/hACE2 triple transgenic mouse colony was established here at the
258 UCI by cross-breeding K18-hACE2 mice (17) with double transgenic HLA-DR*0101/HLA-A*0201 mice
259 (14).

260 The HLA-DR*0101/HLA-A*0201/hACE2 triple transgenic mice were immunized intranasally
261 on day 0 with the multi-epitope coronavirus vaccine at 2×10^{10} viral particles [VP] per mouse, $n = 35$.

262 The vaccine comprised of highly conserved and immunogenic 9 B cell epitopes, 16 CD8⁺ T cell
263 epitopes, and 6 CD4⁺ T cell epitope. Fifteen mice were divided into 3 groups of 5 mice each including
264 the multi-epitope vaccine group, control vaccine group and as a negative control, and the third group
265 of 5 mice received sterile PBS (mock vaccinated group). The triple transgenic mice were intranasally
266 infected with 1×10^4 pfu of SARS-CoV-2 (Delta) delivered in 20 μ L sterile PBS on day 28 following
267 immunization (**Fig. 5A**). Mice were monitored daily for death and weight loss to day 14 post-infection
268 (p.i.) on which they were euthanized for virological and immunological studies.

269 **Virus titration in oropharyngeal swabs:** Throat swabs were analyzed for SARS-CoV-2
270 specific RNA by qRT-PCR. As recommended by the CDC, we used *ORF1ab*-specific primers
271 (forward-5'-CCCTGTGGGTTTTACTTAA-3' and reverse-5'-ACGATTGTGCATCAGCTGA-3') and
272 probe (6FAM-CCGTCTGCGGTATGTGGAAAGGTTATGG-BHQ) to detect the viral RNA level in
273 lungs. Briefly, 5 mL of the total nucleic acid eluate was added to a 20-mL total volume reaction mixture
274 [1 \times TaqPath 1-Step RT-qPCR Master Mix (Thermo Fisher Scientific, Waltham, MA)], with 0.9 mM
275 each primer and 0.2 mM each probe. The qRT-PCR was carried out using the ABI StepOnePlus
276 thermocycler (Life Technologies, Grand Island, NY). When the Ct-value was relatively high ($35 \leq Ct$
277 < 40), the specimen was retested twice and considered positive if the Ct-value of any retest was less
278 than 35.

279 **Statistical analyses:** Data for each differentially expressed markers among blockade-treated
280 and mock-treated groups of HLA-Tg mice were compared by ANOVA and Student t test using
281 GraphPad Prism version 6 (GraphPad Software, La Jolla, CA). Statistical differences observed in the
282 measured Ab responses between healthy donors and COVID-19 patients were calculated using
283 ANOVA and multiple t test comparison procedures in GraphPad Prism. Data are expressed as the mean
284 \pm SD. Results were considered statistically significant at $P < 0.05$.

285

286

287

RESULTS

288

289

1. *Highly conserved B-cell epitopes identified in different SARS-CoV-2 variants of concerns:*

290

291

292

293

294

295

296

297

298

299

300

301

302

303

304

305

306

307

308

309

310

311

A total of 210 COVID-19 patients participated in the study, categorized into asymptomatic and symptomatic groups based on clinical parameters. Blood and nasopharyngeal swabs were collected from all subjects for further analysis. Utilizing a qRT-PCR assay, viral haplotypes unique to different SARS-CoV-2 VOCs were identified. Notably, six novel nonsynonymous mutations ($\Delta 69-70$, $\Delta 242-244$, N501Y, E484K, L452R, and T478K) were employed to differentiate variants including Omicron (B.1.1.529 (BA.1)), Omicron (B.1.1.529 (BA.2)), Alpha (B.1.1.7), Beta (B.1.351), Gamma (P.1), Delta (B.1.617.2), and Epsilon (B.1.427/B.1.429). Serum samples from COVID-19 patients infected with highly pathogenic SARS-CoV-2 VOCs were analyzed for anti-SARS-CoV-2 peptide-specific IgG levels. Graphical representation of optical density revealed the magnitude of IgG response, with dotted lines shown in the graph serve to highlight peptides that consistently exhibit high immunogenicity and stable responses across different SARS-CoV-2 variants of concern, when compared to other conserved peptides (**Fig. S1**). These dotted lines are used to visually emphasize the peptides that elicit stronger and more consistent IgG responses over time, despite the emergence of diverse viral variants compared to their counterparts, providing a clear indication of their reliability and effectiveness in eliciting immune responses. Among the 17 tested peptides (**Supplemental Table 1**), six conserved epitopes ($S_{287-317}$, $S_{369-393}$, $S_{471-501}$, $S_{565-598}$, $S_{614-640}$, $S_{1133-1160}$) were identified as highly immunogenic peptides. These six conserved epitopes exhibited robust immunogenicity and demonstrated conservation across multiple SARS-CoV-2 variants (**Fig. S1**). Sequence homology analysis was conducted to determine the conservancy of immunodominant B-cell epitopes among SARS-CoV-2 variants of concern (**Table. 1**). In parallel, IgG response to conserved ($S_{565-598}$ and $S_{287-317}$), and non-conserved (S_{13-37} and $S_{601-628}$) epitopes was evaluated in COVID-19 patients infected with various SARS-CoV-2 variants demonstrated in the pie charts (**Fig. 3**). The analysis revealed that over time, the immunogenicity of conserved

312 epitopes remained stable and higher compared to non-conserved epitopes. Conversely, the
313 immunogenicity of non-conserved epitopes exhibited a declining trend over time (**Fig. 3**).

314

315 **2. Severity, age, and gender-dependent antibody responses to conserved B-cell epitopes in**

316 **COVID-19 patients:** The immunogenicity of 'universal' B-cell epitopes in COVID-19 patients was
317 examined across different severity groups, age categories, and genders, with a focus on humoral
318 immune responses. ELISA assays were conducted to quantify IgG levels binding to six 'universal' B-
319 cell epitopes in COVID-19 patient sera. Analysis revealed significant variations between asymptomatic
320 and symptomatic individuals across all six peptides of interest (**Fig. S2A**). Notably, asymptomatic
321 patients exhibited higher IgG binding levels of the six conserved epitopes (**Figs. 4A and S2A**) compared
322 to symptomatic patients, indicating a more robust humoral immune response in asymptomatic cases
323 (**Fig. 4A**). All the six tested peptides showed significant IgG binding levels across the VOCs studied,
324 highlighting their conserved immunogenicity (**Figs. 4A, S2A, S3A, and S4A**). Neutralization assays
325 were performed to evaluate the neutralization efficiency of sera from asymptomatic and symptomatic
326 COVID-19 patients against the different SARS-CoV-2 VOCs (**Figs. 4B, S2B, S3B, and S4B**). The
327 results demonstrated notable differences in neutralization percentages between severity groups and
328 across various VOCs. Specifically, sera from asymptomatic patients exhibited higher neutralizing
329 antibody titers compared to sera from symptomatic patients, indicating a more potent neutralizing
330 activity in asymptomatic cases (**Figs. 4B, S2B, S3B, and S4B**). In terms of age-dependent immune
331 responses, significantly higher IgG binding levels were observed among young individuals compared
332 to older individuals across all six peptides of interest (**Figs. 4A, S2A, S3A, and S4A**). Moreover, a
333 significant increase in IgG binding levels was observed in each of the six peptides across different
334 SARS-CoV-2 variants of concern (**Figs. 4A, S2A, S3A, and S4A**). Neutralization assays were
335 conducted to assess the neutralization efficiency of young COVID-19 patient sera compared to old
336 COVID-19 patient sera against the different SARS-CoV-2 variants of concern. The results indicated
337 notable differences in neutralization percentages between age groups and across various VOCs, with

338 young individuals demonstrating significantly higher neutralizing antibody titers compared to older
339 individuals (**Figs. 4B, S2B, S3B and S4B**). Regarding gender-dependent immune responses, analysis
340 of IgG binding levels revealed no significant differences between male and female patients across all
341 six peptides of interest (**Figs. 4A, S2A, S3A, and S4A**). Similarly, neutralization assays showed
342 comparable neutralization percentages between male and female patients against different VOCs
343 (**Figs. 4B, S2B, S3B and S4B**).

344

345 **3. Conserved human B epitopes protect against infection and COVID-19-Like symptoms**
346 **caused by SARS-CoV-2 delta variant of concern in HLA-DR0101/HLA-A0201/hACE2 triple**
347 **transgenic mice:** Triple transgenic HLA-A02:01/HLA-DRB101:01-hACE-2 mice were intranasally
348 vaccinated with two different AAV9-based Coronavirus vaccines: multiepitope vaccine containing 8
349 conserved B cell epitopes and control vaccine containing six B cell epitopes, along with a Mock
350 vaccinated control group. ELISA and FFA assays were performed 26 days post-immunization, followed
351 by intranasal challenge with SARS-CoV-2 Delta variant. Mice were monitored for weight loss, survival,
352 and viral titer over 14 days post-challenge.

353 As illustrated in **Fig. 5B**, we observed significant protection against weight loss in the mice
354 vaccinated with multiepitope vaccine compared to control vaccine and to the Mock vaccinated group.
355 Additionally, a higher percentage of multiepitope vaccinated mice survived the challenge compared to
356 the control vaccine and mock vaccinated group (**Fig. 5C**). Viral titration data demonstrated a marked
357 decrease in viral RNA copy number in the nasopharyngeal swabs of mice vaccinated with multiepitope
358 vaccine at days 2, 6, 10, and 14 post-challenge in comparison with control vaccine and the mock
359 vaccinated group (**Fig. 5D**). ELISA results indicated a robust IgG binding affinity specific for the 6
360 "universal" B cell epitopes and the spike protein in mice vaccinated with multiepitope vaccine compared
361 to control vaccine and mock vaccinated group (**Fig. 5E**). We also found a higher neutralization
362 percentage in sera from mice vaccinated with multiepitope vaccine against Alpha, Beta, Epsilon, Delta,
363 and Omicron variants compared to the control vaccine and Mock vaccinated group (**Fig. 5F**).

364

DISCUSSION

365

366 Since the emergence of SARS-CoV-2 in late 2019, the identification and understanding of B cell
367 epitopes have become pivotal in the development of effective vaccines and therapeutic strategies
368 against COVID-19. B cell epitopes, which are specific regions on antigens recognized by antibodies,
369 play a crucial role in mediating the neutralization of the virus. The continuous emergence of SARS-CoV-
370 2 variants, including the recent Omicron sub-variants, has complicated efforts to control the COVID-19
371 pandemic. Despite the significant impact of Spike-based COVID-19 vaccines, their effectiveness against
372 newer variants is waning (19, 20), underscoring the pressing need for a next-generation SARS-CoV-2
373 vaccine that contains a repertoire of conserved B cell epitopes. The exploration of conserved B cell
374 epitopes in a universal coronavirus vaccine offers a promising path to enhancing immunity against the
375 multitude of SARS-CoV-2 variants and sub-variants, thereby potentially attenuating the persistent threat
376 posed by the pandemic.

377 B cell epitopes are short sequences or structures on an antigen recognized by antibodies
378 produced by B cells. Neutralization occurs when these antibodies bind to viral epitopes and block the
379 virus from entering host cells. For SARS-CoV-2, the primary target of neutralizing antibodies is the spike
380 (S) protein, which facilitates viral entry into human cells by binding to the ACE2 receptor (21). The spike
381 protein of SARS-CoV-2 is composed of two subunits: S1 and S2. The S1 subunit includes the receptor-
382 binding domain (RBD), which is a major B cell epitope. Antibodies targeting the RBD are highly effective
383 at neutralizing the virus because they prevent the spike protein from interacting with the ACE2 receptor
384 (22). Other important epitopes include the N-terminal domain (NTD) of the S1 subunit and the S2
385 subunit, although the RBD remains the primary focus for neutralizing responses (23-25). However, it
386 was noticed that the emerging variants of SARS-CoV-2 plays a role in B cell epitope recognition. Since
387 2019, SARS-CoV-2 has undergone several mutations, leading to the emergence of new variants with
388 changes in the spike protein. These variants, including Alpha, Beta, Delta, and Omicron, have
389 introduced mutations in the RBD and other regions, potentially altering the B cell epitopes (26). For

390 instance, the Omicron variant has multiple mutations in the RBD, which can reduce the effectiveness of
391 antibodies generated by previous infection or vaccination (27). Understanding these changes is crucial
392 for maintaining vaccine efficacy and developing new therapeutic strategies.

393 The design of COVID-19 vaccines has been heavily influenced by the need to elicit a strong
394 antibody response against key B cell epitopes. mRNA vaccines, such as those developed by Pfizer-
395 BioNTech and Moderna, encode the spike protein and stimulate an immune response targeting the RBD
396 (28-30). Viral vector vaccines, like AstraZeneca's, also focus on the spike protein but use a different
397 delivery mechanism. The effectiveness of these vaccines in neutralizing SARS-CoV-2 largely depends
398 on the ability of the induced antibodies to recognize and bind to critical epitopes on the spike protein
399 (31). Several studies regarding the effectiveness of the current modified messenger RNA (mRNA)
400 vaccines indicate that these vaccines had reduced levels of neutralizing antibodies against recent
401 SARS-CoV-2 variants compared to earlier variants (19, 32). In this report, we have identified 6 conserved
402 B-cell epitopes among all known SARS-CoV-2 variants, previous SARS and MERS coronavirus strains,
403 and strains specific to different species that were reported to be hosts for SARS/MERS (bat, civet cat,
404 pangolin, and camel). In this study, we used a combination of these highly conserved B cell epitopes
405 and incorporated them in a multi-epitope pan-variant SARS-CoV-2 vaccine that contain CD8⁺ and CD4⁺
406 T- and B- cell epitopes.

407 We demonstrated that among the seventeen conserved B-cell epitopes, six (S₂₈₇₋₃₁₇, S₃₆₉₋₃₉₃,
408 S₄₇₁₋₅₀₁, S₅₆₅₋₅₉₈, S₆₁₄₋₆₄₀, S₁₁₃₃₋₁₁₆₀) were highly immunogenic. The magnitude of IgG response
409 consistently of these six peptides exhibit high immunogenicity and stable responses across different
410 SARS-CoV-2 VOCs, when compared to other conserved peptides. Suggesting that these peptides elicit
411 stronger and more consistent IgG responses over time, despite the emergence of diverse viral variants
412 compared to their counterparts, providing a clear indication of their reliability and effectiveness in eliciting
413 immune responses. These epitopes exhibited robust immunogenicity and demonstrated conservation
414 across multiple SARS-CoV-2 variants. This analysis revealed that over time, the immunogenicity of
415 conserved epitopes remained stable and higher compared to non-conserved epitopes. Conversely, the

416 immunogenicity of non-conserved epitopes exhibited a declining trend over time. Upon selecting six
417 conserved epitopes ($S_{287-317}$, $S_{369-393}$, $S_{471-501}$, $S_{565-598}$, $S_{614-640}$, $S_{1133-1160}$) as highly immunogenic peptides,
418 we subsequently placed additional focus on these peptides and correlated their IgG level with severity,
419 age, and gender. Notably, asymptomatic patients showed a significantly higher IgG binding levels to the
420 six conserved epitopes ($S_{287-317}$, $S_{369-393}$, $S_{471-501}$, $S_{565-598}$, $S_{614-640}$, $S_{1133-1160}$) across different SARS-CoV-
421 2 VOCs Alpha (B.1.1.7), Beta (B.1.351), Gamma (P.1), Delta (B.1.617.2), Omicron (BA.1) and Omicron
422 (BA.2) when compared to symptomatic patients. Furthermore, when investigating the neutralization
423 levels using sera from asymptomatic and symptomatic individuals across various VOCs, we also
424 demonstrated that sera from asymptomatic patients exhibited higher neutralizing antibody titers
425 compared to sera from symptomatic patients, indicating a more potent neutralizing activity in
426 asymptomatic. Our studies suggest a potential correlation between elevated IgG levels specific to
427 certain peptides and increased neutralization activity in asymptomatic individuals, pointing towards a
428 more robust immune response in this cohort. Altogether, these findings imply that the magnitude of the
429 peptide-specific IgG response may influence the ability to neutralize the virus, highlighting the
430 importance of further exploring this relationship in understanding COVID-19 pathogenesis and immune
431 response dynamics.

432 This study investigated age-related immune responses and found a trend of significantly higher
433 IgG binding levels among younger individuals in comparison to their older counterparts across all six
434 peptides examined suggesting a potential age-dependent variation in the humoral immune response to
435 SARS-CoV-2 infection, with younger individuals exhibiting a more robust antibody response to the viral
436 epitopes of interest. Furthermore, our analysis revealed a consistent increase in IgG binding levels
437 across all six peptides when considering different VOCs of SARS-CoV-2. This observation indicates that
438 the epitopes targeted by these antibodies remain immunogenic and conserved across various viral
439 strains, underscoring their potential significance as vaccine targets against evolving viral variants. To
440 further assess the functional relevance of these age-related differences in antibody responses, we
441 conducted neutralization assays using sera from young and old COVID-19 patients against different

442 VOCs of SARS-CoV-2. Notable increases were observed in neutralization efficiency between age
443 groups and across various viral variants. Specifically, young individuals exhibited significantly higher
444 neutralizing antibody titers compared to their older counterparts, indicating a potential age-associated
445 variation in the ability to neutralize the virus. These findings suggest that age may play a critical role in
446 shaping the magnitude and efficacy of the humoral immune response to SARS-CoV-2 infection.
447 Understanding these age-related differences in immune responses could have important implications
448 for vaccine design and prioritization, as well as for informing strategies aimed at enhancing vaccine
449 efficacy across different age demographics. Further research is warranted to elucidate the underlying
450 mechanisms driving these age-dependent variations in immune responses and to assess their
451 implications for COVID-19 disease severity and vaccine effectiveness. In examining gender-dependent
452 immune responses, our analysis of IgG binding levels across the six peptides of interest revealed no
453 significant differences between male and female patients. Similarly, we observed comparable
454 neutralization percentages between male and female patients across different VOCs when performing
455 neutralization assays to evaluate the efficacy of neutralizing antibodies. This study further suggests that
456 gender may not be a significant factor influencing the humoral immune response to SARS-CoV-2
457 infection, at least in terms of IgG binding and neutralizing antibody titers.

458 After identifying six highly conserved epitopes ($S_{287-317}$, $S_{369-393}$, $S_{471-501}$, $S_{565-598}$, $S_{614-640}$, S_{1133-}
459 $_{1160}$), we evaluated the in vivo efficacy of a multiepitope vaccine incorporating these highly conserved B
460 cell epitopes along with $CD4^+$ T cell and $CD8^+$ T cell epitopes using a triple transgenic HLA-A02:01/HLA-
461 *DRB101:01-hACE-2* mouse model. Our findings demonstrated significant protective effects of the
462 multiepitope vaccine against SARS-CoV-2 (Delta variant) challenge. Mice immunized with the
463 multiepitope vaccine showed substantial protection against weight loss and death. The weight loss and
464 survival found herein agree with previous reports in the context to Delta (B.1.617.2) (33). Viral titration
465 analysis revealed a significant reduction in viral RNA copy numbers in the nasopharyngeal swabs of
466 mice vaccinated with the multiepitope vaccine at various time points post-challenge (days 2, 6, 10, and
467 14). This indicates effective viral clearance in vaccinated mice compared to the control groups.

468 Furthermore, ELISA results demonstrated robust IgG binding affinity specific to the six "universal" B cell
469 epitopes and the spike protein in mice vaccinated with the multiepitope vaccine. Importantly, we
470 observed a higher neutralization percentage in sera from mice vaccinated with the multiepitope vaccine
471 against various SARS-CoV-2 variants, including Alpha, Beta, Epsilon, Delta, and Omicron, compared to
472 the control groups. This highlights the vaccine's ability to induce a strong humoral immune response
473 targeting conserved epitopes underscoring the potential of the multiepitope vaccine to confer broad
474 protection against emerging VOCs. Overall, our results demonstrate the promising efficacy of the
475 multiepitope vaccine in providing protection against SARS-CoV-2 infection and highlight its potential as
476 a candidate for further preclinical and clinical development.

477 There are several studies on epitope profiling in existing COVID-19 mRNA vaccines (34, 35).
478 One study mapped immunogenic amino acid motifs and linear epitopes of the primary sequence of the
479 SARS-CoV-2 spike protein that induce IgG in recipients of the Pfizer-BioNTech COVID-19 mRNA
480 vaccine (34). The data revealed various distinctive amino acid motifs recognized by vaccine-elicited IgG,
481 some of which mimic three-dimensional conformation (mimotopes) and are identical to dominant linear
482 epitopes in the C-terminal region of the spike protein observed in SARS-CoV, bat coronaviruses, and
483 epitopes triggering IgG during natural infection. However, these epitopes have limited homology to the
484 spike protein of non-pathogenic human coronaviruses (34). Another study highlighted high-resolution
485 linear epitope profiling of Pfizer-BioNTech COVID-19 mRNA vaccine recipients and COVID-19 patients
486 showed that vaccine-induced antibodies targeting the viral spike receptor-binding domain (RBD) have
487 a broader distribution across the RBD compared to antibodies induced by natural infection (35).
488 Furthermore, mutation panel assays targeting viral variants of concern demonstrated that the epitope
489 repertoire induced by the mRNA vaccine is rich in breadth, potentially conferring resistance against viral
490 evolutionary escapes in the future. This represents a significant advantage of vaccine-induced immunity
491 (35). The identified epitopes in COVID-19 mRNA vaccines may serve as a basis for further research on
492 immune escape, viral variants, and the design of vaccines and therapies.

493 SARS-CoV-2 shares sequence, structural, and functional homology with SARS-CoV and MERS-
494 CoV (36). Antibodies against SARS-CoV spike protein can inhibit SARS-CoV-2 binding to ACE2 (37).
495 The spike protein, vital for receptor binding, possesses conserved sequences and high immunogenicity,
496 making it a priority in COVID-19 vaccine development. Out of the current clinical vaccine candidates,
497 32% are recombinant protein vaccines, while RNA vaccines, viral vector-based vaccines, and
498 inactivated virus vaccines account for 23%, 13%, and 13% respectively (38, 39). Many of these
499 candidates use either full-length spike protein or only parts from the spike protein various lengths of the
500 receptor-binding domain (RBD) to induce potent neutralizing antibody responses. However, it is
501 important to note that mutations in spike protein can impact the effectiveness of those COVID-19
502 vaccines based only on the spike protein (36). Ongoing research aims to identify additional B cell
503 epitopes and understand their role in neutralization, especially in the context of evolving variants. This
504 includes studying the cross-reactivity of antibodies and the development of broadly neutralizing
505 antibodies that can target conserved regions of the spike protein across different variants (40, 41).
506 Advances in structural biology and immunology will continue to enhance our understanding of B cell
507 epitopes and their role in combating SARS-CoV-2. Understanding the role of B cell epitopes in
508 neutralizing SARS-CoV-2 is crucial for ongoing efforts to control the pandemic. Continued research into
509 these epitopes will be vital for adapting vaccines and treatments to effectively address emerging variants
510 and ensure robust protection against COVID-19.

511 The threat of COVID-19 still remains serious, with persistently high rates of illness and mortality
512 worldwide. Our findings underscore the efficacy and potential of a multiepitope vaccine designed to
513 target conserved B-cell epitopes as well as CD4⁺ and CD8⁺ T cell epitopes. Our strategy of incorporating
514 selected highly conserved B cell epitopes into COVID-19 vaccines presents a pivotal approach in the
515 fight against emerging variants. By putting to use the power of both humoral and cellular immunity, a
516 multiepitope vaccines hold significant promise and provides a broader and more durable protection
517 against multiple SARS-CoV-2 variants. This investigation highlights the importance of incorporating B-

518 cell epitopes into next-generation vaccine strategies for enhanced protection against evolving viral

519 threats.

520

521

522

ACKNOWLEDGMENTS

523 This work is supported by the Fast-Grant PR12501 from Emergent Ventures, by a Gavin Herbert
524 Eye Institute internal grant, by Public Health Service Research grants AI158060, AI174383, AI150091,
525 AI143348, AI147499, AI143326, AI138764, AI124911, and AI110902 from the National Institutes of
526 Allergy and Infectious Diseases (NIAID) to LBM.

527

528

529

530

531

532

533

534

535

536

537

538

REFERENCES

- 539 1. Prakash S, Srivastava R, Coulon PG, Dhanushkodi NR, Chentoufi AA, Tifrea DF, et al. Genome-
540 Wide B Cell, CD4(+), and CD8(+) T Cell Epitopes That Are Highly Conserved between Human and
541 Animal Coronaviruses, Identified from SARS-CoV-2 as Targets for Preemptive Pan-Coronavirus
542 Vaccines. *J Immunol.* 2021;206(11):2566-82.
- 543 2. Prakash S, Dhanushkodi NR, Zayou L, Ibraim IC, Quadiri A, Coulon PG, et al. Cross-Protection
544 Induced by Highly Conserved Human B, CD4 (+), and CD8 (+) T Cell Epitopes-Based Coronavirus
545 Vaccine Against Severe Infection, Disease, and Death Caused by Multiple SARS-CoV-2 Variants of
546 Concern. *Frontiers In Immunology.* 2024;29(12):45-56.
- 547 3. Pedersen SF, Ho YC. SARS-CoV-2: A Storm is Raging. *J Clin Invest.* 2020.
- 548 4. Bellocchi MC, Scutari R, Carioti L, Iannetta M, Marchegiani G, Piermatteo L, et al. Frequency of
549 Atypical Mutations in the Spike Glycoprotein in SARS-CoV-2 Circulating from July 2020 to July 2022 in
550 Central Italy: A Refined Analysis by Next Generation Sequencing. *Viruses.* 2023;15(8).
- 551 5. Desmecht S, Tashkeev A, El Moussaoui M, Marechal N, Peree H, Tokunaga Y, et al. Kinetics
552 and Persistence of the Cellular and Humoral Immune Responses to BNT162b2 mRNA Vaccine in
553 SARS-CoV-2-Naive and -Experienced Subjects: Impact of Booster Dose and Breakthrough Infections.
554 *Front Immunol.* 2022;13:863554.
- 555 6. Sharma S, Vercruyssen T, Sanchez-Felipe L, Kerstens W, Rasulova M, Bervoets L, et al.
556 Updated vaccine protects against SARS-CoV-2 variants including Omicron (B.1.1.529) and prevents
557 transmission in hamsters. *Nat Commun.* 2022;13(1):6644.
- 558 7. Washington NL, Gangavarapu K, Zeller M, Bolze A, Cirulli ET, Schiabor Barrett KM, et al.
559 Emergence and rapid transmission of SARS-CoV-2 B.1.1.7 in the United States. *Cell.*
560 2021;184(10):2587-94 e7.

- 561 8. Liu H, Iketani S, Zask A, Khanizeman N, Bednarova E, Forouhar F, et al. Development of
562 optimized drug-like small molecule inhibitors of the SARS-CoV-2 3CL protease for treatment of COVID-
563 19. *Nat Commun.* 2022;13(1):1891.
- 564 9. Konings F, Perkins MD, Kuhn JH, Pallen MJ, Alm EJ, Archer BN, et al. SARS-CoV-2 Variants
565 of Interest and Concern naming scheme conducive for global discourse. *Nat Microbiol.* 2021;6(7):821-
566 3.
- 567 10. Kumar S, Thambiraja TS, Karuppanan K, Subramaniam G. Omicron and Delta variant of SARS-
568 CoV-2: A comparative computational study of spike protein. *J Med Virol.* 2022;94(4):1641-9.
- 569 11. Park T, Hwang H, Moon S, Kang SG, Song S, Kim YH, et al. Vaccines against SARS-CoV-2
570 variants and future pandemics. *Expert Rev Vaccines.* 2022;21(10):1363-76.
- 571 12. Evans JP, Liu SL. Challenges and Prospects in Developing Future SARS-CoV-2 Vaccines:
572 Overcoming Original Antigenic Sin and Inducing Broadly Neutralizing Antibodies. *J Immunol.*
573 2023;211(10):1459-67.
- 574 13. Lyke KE, Atmar RL, Islas CD, Posavad CM, Szydlo D, Paul Chourdury R, et al. Rapid decline
575 in vaccine-boosted neutralizing antibodies against SARS-CoV-2 Omicron variant. *Cell Rep Med.*
576 2022;3(7):100679.
- 577 14. Shi J, Zheng J, Zhang X, Tai W, Compas R, Deno J, et al. A T cell-based SARS-CoV-2 spike
578 protein vaccine provides protection without antibodies. *JCI Insight.* 2024;9(5).
- 579 15. Gatz SA, Pohla H, Schendel DJ. A PCR-SSP method to specifically select HLA-A*0201
580 individuals for immunotherapeutic studies. *Tissue antigens.* 2000;55(6):532-47.
- 581 16. Olerup O, Zetterquist H. HLA-DRB1*01 subtyping by allele-specific PCR amplification: a
582 sensitive, specific and rapid technique. *Tissue antigens.* 1991;37(5):197-204.
- 583 17. Buchfink B, Reuter K, Drost HG. Sensitive protein alignments at tree-of-life scale using
584 DIAMOND. *Nat Methods.* 2021;18(4):366-8.

- 585 18. Wang H, Jean S, Eltringham R, Madison J, Snyder P, Tu H, et al. Mutation-Specific SARS-CoV-
586 2 PCR Screen: Rapid and Accurate Detection of Variants of Concern and the Identification of a Newly
587 Emerging Variant with Spike L452R Mutation. *J Clin Microbiol.* 2021;59(8):e0092621.
- 588 19. Duchene S, Featherstone L, Haritopoulou-Sinanidou M, Rambaut A, Lemey P, Baele G.
589 Temporal signal and the phylodynamic threshold of SARS-CoV-2. *Virus Evol.* 2020;6(2):veaa061.
- 590 20. Rubin R. COVID-19 Vaccines vs Variants-Determining How Much Immunity Is Enough. *JAMA.*
591 2021;325(13):1241-3.
- 592 21. Hoffmann M, Kleine-Weber H, Schroeder S, Kruger N, Herrler T, Erichsen S, et al. SARS-CoV-
593 2 Cell Entry Depends on ACE2 and TMPRSS2 and Is Blocked by a Clinically Proven Protease Inhibitor.
594 *Cell.* 2020;181(2):271-80 e8.
- 595 22. Barton MI, MacGowan SA, Kutuzov MA, Dushek O, Barton GJ, van der Merwe PA. Effects of
596 common mutations in the SARS-CoV-2 Spike RBD and its ligand, the human ACE2 receptor on binding
597 affinity and kinetics. *Elife.* 2021;10.
- 598 23. Liu L, Iketani S, Guo Y, Chan JF, Wang M, Liu L, et al. Striking antibody evasion manifested by
599 the Omicron variant of SARS-CoV-2. *Nature.* 2022;602(7898):676-81.
- 600 24. Liu L, Wang P, Nair MS, Yu J, Rapp M, Wang Q, et al. Potent neutralizing antibodies against
601 multiple epitopes on SARS-CoV-2 spike. *Nature.* 2020;584(7821):450-6.
- 602 25. Carabelli AM, Peacock TP, Thorne LG, Harvey WT, Hughes J, Consortium C-GU, et al. SARS-
603 CoV-2 variant biology: immune escape, transmission and fitness. *Nat Rev Microbiol.* 2023;21(3):162-
604 77.
- 605 26. Planas D, Veyer D, Baidaliuk A, Staropoli I, Guivel-Benhassine F, Rajah MM, et al. Reduced
606 sensitivity of SARS-CoV-2 variant Delta to antibody neutralization. *Nature.* 2021;596(7871):276-80.
- 607 27. Chen RE, Zhang X, Case JB, Winkler ES, Liu Y, VanBlargan LA, et al. Resistance of SARS-
608 CoV-2 variants to neutralization by monoclonal and serum-derived polyclonal antibodies. *Nat Med.*
609 2021;27(4):717-26.

- 610 28. Cele S, Gazy I, Jackson L, Hwa SH, Tegally H, Lustig G, et al. Escape of SARS-CoV-2 501Y.V2
611 from neutralization by convalescent plasma. *Nature*. 2021;593(7857):142-6.
- 612 29. El Sahly HM, Baden LR, Essink B, Doblecki-Lewis S, Martin JM, Anderson EJ, et al. Efficacy of
613 the mRNA-1273 SARS-CoV-2 Vaccine at Completion of Blinded Phase. *The New England journal of*
614 *medicine*. 2021;385(19):1774-85.
- 615 30. Polack FP, Thomas SJ, Kitchin N, Absalon J, Gurtman A, Lockhart S, et al. Safety and Efficacy
616 of the BNT162b2 mRNA Covid-19 Vaccine. *The New England journal of medicine*. 2020;383(27):2603-
617 15.
- 618 31. Slaoui M, Hepburn M. Developing Safe and Effective Covid Vaccines - Operation Warp Speed's
619 Strategy and Approach. *N Engl J Med*. 2020;383(18):1701-3.
- 620 32. Hao L, Hsiang TY, Dalmat RR, Ireton R, Morton JF, Stokes C, et al. Dynamics of SARS-CoV-2
621 VOC Neutralization and Novel mAb Reveal Protection against Omicron. *Viruses*. 2023;15(2).
- 622 33. Prakash S, Dhanushkodi NR, Zayou L, Ibraim IC, Quadiri A, Coulon PG, et al. Cross-protection
623 induced by highly conserved human B, CD4(+), and CD8(+) T-cell epitopes-based vaccine against
624 severe infection, disease, and death caused by multiple SARS-CoV-2 variants of concern. *Front*
625 *Immunol*. 2024;15:1328905.
- 626 34. Amanat F, Thapa M, Lei T, Ahmed SMS, Adelsberg DC, Carreño JM, et al. SARS-CoV-2 mRNA
627 vaccination induces functionally diverse antibodies to NTD, RBD, and S2. *Cell*. 2021;184(15):3936-
628 48.e10.
- 629 35. Nitahara Y, Nakagama Y, Kaku N, Candray K, Michimuko Y, Tshibangu-Kabamba E, et al. High-
630 Resolution Linear Epitope Mapping of the Receptor Binding Domain of SARS-CoV-2 Spike Protein in
631 COVID-19 mRNA Vaccine Recipients. *Microbiol Spectr*. 2021;9(3):e0096521.
- 632 36. Wu A, Peng Y, Huang B, Ding X, Wang X, Niu P, et al. Genome Composition and Divergence
633 of the Novel Coronavirus (2019-nCoV) Originating in China. *Cell Host Microbe*. 2020;27(3):325-8.
- 634 37. Salvatori G, Luberto L, Maffei M, Aurisicchio L, Roscilli G, Palombo F, Marra E. SARS-CoV-2
635 SPIKE PROTEIN: an optimal immunological target for vaccines. *J Transl Med*. 2020;18(1):222.

- 636 38. Liang JG, Su D, Song TZ, Zeng Y, Huang W, Wu J, et al. S-Trimer, a COVID-19 subunit vaccine
637 candidate, induces protective immunity in nonhuman primates. *Nat Commun.* 2021;12(1):1346.
- 638 39. Nelde A, Bilich T, Heitmann JS, Maringer Y, Salih HR, Roerden M, et al. SARS-CoV-2-derived
639 peptides define heterologous and COVID-19-induced T cell recognition. *Nat Immunol.* 2020.
- 640 40. Li Y, Xu Z, Lei Q, Lai DY, Hou H, Jiang HW, et al. Antibody landscape against SARS-CoV-2
641 reveals significant differences between non-structural/accessory and structural proteins. *Cell Rep.*
642 2021;36(2):109391.
- 643 41. Qi H, Liu B, Wang X, Zhang L. The humoral response and antibodies against SARS-CoV-2
644 infection. *Nat Immunol.* 2022;23(7):1008-20.
- 645

646

FIGURE LEGENDS

647

648 **Figure 1. Assessment of SARS-CoV-2 infection severity and immune response:**

649 Experimental plan outlines the assessment of SARS-CoV-2 infection severity and immune response in
650 a cohort of 198 patients, comprising both asymptomatic and symptomatic individuals presenting to the
651 clinic with varying degrees of COVID-19 symptoms. Additionally, 12 healthy controls are included for
652 comparative analysis. The patient cohort is categorized into asymptomatic (ASYMP) and symptomatic
653 (SYMP) groups, with severity levels ranging from 0 to 5 based on symptom severity and clinical
654 outcomes. Asymptomatic individuals exhibit no symptoms, while symptomatic patients are further
655 classified based on the severity of their symptoms, hospital admission, ICU admission, ventilation
656 support, and mortality. Blood and nasopharyngeal swabs are collected from both symptomatic (n = 85)
657 and asymptomatic (n = 113) patients for subsequent analysis. Patients are classified based on the
658 detection of 7 SARS-CoV-2 variants of concern using qPCR from nasopharyngeal swabs, as well as
659 their disease severity, age, and gender. Serum IgG and neutralizing antibody levels are measured in
660 symptomatic (n = 85), and asymptomatic (n = 109) patients infected with different SARS-CoV-2 variants
661 using enzyme-linked immunosorbent assay (ELISA) and neutralization assays on serum samples.

662

663 **Figure 2. Sequence homology analysis of immunodominant B cell epitopes among SARS-**

664 **CoV-2 variants of concern:** The figure represents the results of sequence homology analysis to assess
665 the degree of conservancy of immunodominant B cell epitopes among SARS-CoV-2 variants of
666 concern. Seventeen peptides, identified as potential B cell epitopes, were subjected to analysis, and
667 categorized into conserved epitopes and non-conserved epitopes based on sequence similarity across
668 different variants. Conserved epitopes exhibit a high degree of sequence conservation among variants,
669 suggesting potential cross-reactivity and broad immune recognition. Non-conserved epitopes, on the

670 other hand, show variability in sequence composition across variants, indicating potential immune
671 evasion and reduced recognition by antibodies.

672

673 **Figure 3. IgG Response to conserved and non-conserved epitopes in COVID-19 patients**

674 ***infected with different SARS-CoV-2 variants:*** The figure displays six pie charts representing the IgG
675 response to S₅₆₅₋₅₉₈ and S₁₃₋₃₇ epitopes (upper panel) and S₂₈₇₋₃₁₇ and S₆₀₁₋₆₂₈ (bottom panel) in COVID-
676 19 patients infected with various SARS-CoV-2 variants of concern. Each pie chart corresponds to a
677 specific variant, including Alpha, Beta, Gamma, Delta, Omicron BA.1, and Omicron BA.2, which
678 appeared at different time points during the pandemic. In each pie chart, black segments represent the
679 IgG response against conserved peptide sequences (S₅₆₅₋₅₉₈ and S₂₈₇₋₃₁₇), while white segments
680 represent the IgG response against non-conserved peptide sequences (S₁₃₋₃₇ and S₆₀₁₋₆₂₈). The intensity
681 of the black and white segments indicates the relative magnitude of the IgG response to conserved and
682 non-conserved epitopes, respectively.

683

684 **Figure 4. IgG levels and neutralization percentages in COVID-19 patients: a comparative**

685 ***analysis by ELISA and Neutralization Assay across severity, age, and gender groups:*** (A) IgG
686 Response to Conserved Peptide in COVID-19 Patients are shown in *panel A*. The upper pie chart
687 displays the IgG levels against a conserved peptide in symptomatic (steel) and asymptomatic (white)
688 COVID-19 patients infected with six different SARS-CoV-2 variants of concern: Alpha, Beta, Gamma,
689 Delta, Omicron BA.1, and Omicron BA.2. The middle pie chart shows the IgG levels against the
690 conserved peptide in young (nickel) and old (white) COVID-19 patients infected with the same variants.
691 The bottom pie chart represents the IgG levels against the conserved peptide in female (magnesium)
692 and male (white) COVID-19 patients infected with the same variants. (B) Panel shows neutralization
693 percent in COVID-19 patients. The upper panel illustrates the neutralization percentages in
694 asymptomatic versus symptomatic COVID-19 patients against the Washington and Omicron BA.2
695 variants. The middle panel depicts the neutralization percentages in young and old COVID-19 patients

696 against the same variants. The bottom panel displays the neutralization percentages in female and
697 male COVID-19 patients against the same variants.

698

699 **Figure 5. The effect of immunization with Adeno-Associated Virus 9 based multiepitope-**
700 **Coronavirus vaccine incorporating conserved human B cell epitopes on COVID-19-like**
701 **symptoms detected from triple transgenic HLA-A*02:01/HLA-DRB1*01:01-hACE-2 mice and**
702 **infected with highly pathogenic SARS-CoV-2 Delta variant of concern: (A)** Experimental plan to
703 study the effect of vaccination in triple transgenic HLA-A*02:01/HLA-DRB1*01:01-hACE-2 mice. On day
704 0 Triple transgenic HLA-A*02:01/HLA-DRB1*01:01-hACE-2 mice (7-8-week-old, $n = 15$) were
705 vaccinated intranasally with two different AAV9 based multiepitope vaccines 2×10^{10} Viral Particle per
706 vaccine per mouse named as multiepitope vaccine containing 8 conserved B cell epitopes ($n = 5$),
707 control vaccine containing 6 B cell epitopes ($n = 5$) and finally Mock vaccinated group that received
708 1XPBS ($n = 5$) were used as control. At day 26 post immunization the blood was drawn for ELISA and
709 FFA and two days later mice intranasally challenged with 20ul of SARS-CoV-2 Delta (B.1.617.2) variant
710 of concern at 1×10^4 pfu. Mice were followed for weight loss, survival, and viral titer for 14 days. **(B)** Data
711 showing average percent weight change each day post immunization to the body weight on the day of
712 infection. **(C)** shows the percentage survival detected in mice groups that received either multiepitope
713 vaccine or control vaccine and finally the mock vaccinated group. **(D)** Viral titration data showing viral
714 RNA copy number in the nasopharyngeal swabs of each group at days 2, 6, 10 and 14 post challenge
715 Delta (B.1.617.2) variant. The IgG binding affinity specific for 6 “universal” B cell epitopes as well as the
716 spike protein measured by ELISA are shown in *panel (E)*. The **(F)** *panel* represents neutralization
717 percent by sera from mice that were given multiepitope vaccine, control vaccine or Mock vaccinated
718 group against Alpha (B.1.1.7), Beta (B.1.351), Epsilon (B.1.427/B.1.429), Delta (B.1.617.2), and
719 Omicron (XBB1.5). Bars represent means \pm SEM. P values are calculated using unpaired t -test,
720 comparing results obtained in vaccinated vs. mock-vaccinated mice.

721

722 **Table 1. SARS-CoV-2 variant screening in COVID-19 patients:** The table represents the
723 distribution of SARS-CoV-2 variants detected in 198 COVID-19 positive patients using TaqMan
724 quantitative polymerase reaction (qRT-PCR) assays. Variants were identified based on 6 specific
725 nonsynonymous mutations associated with each variant, including $\Delta 69-70$, $\Delta 242-244$, S-501Y, S-
726 484K, and S-452R, among others. Samples showing positive results for variant-specific mutations
727 highlighted in black were considered screen positive and assigned to the respective variant group.

728
729 **Table 2. Screening COVID-19 patients involved assessing SARS-CoV-2 variants, age,**
730 **gender, and severity:** Screening process of COVID-19 patients ($n = 210$) into Asymptomatic ($n = 113$)
731 and Symptomatic ($n = 85$) categories based on clinical parameters. the groups were segregated based
732 on gender into females ($n = 96$) and males ($n = 102$), as well as based on age into young (age between
733 19 and 49 years old) individuals ($n = 111$) and old (age between 50 and 89 years old) individuals ($n =$
734 87). Blood and nasopharyngeal swabs were collected from all the subjects and a qRT-PCR assay was
735 performed. Six novel nonsynonymous mutations ($\Delta 69-70$, $\Delta 242-244$, N501Y, E484K, L452R, and
736 T478K) were used to identify the haplotypes unique to different SARS-CoV-2 variants of concern
737 (Omicron (B.1.1.529 (BA.1)), Omicron (B.1.1.529 (BA.2)), Alpha (B.1.1.7), Beta (B.1.351), Gamma
738 (P.1), Delta (B.1.617.2), and Epsilon (B.1.427/B.1.429)).

739

740

741

742

743

744

745

746

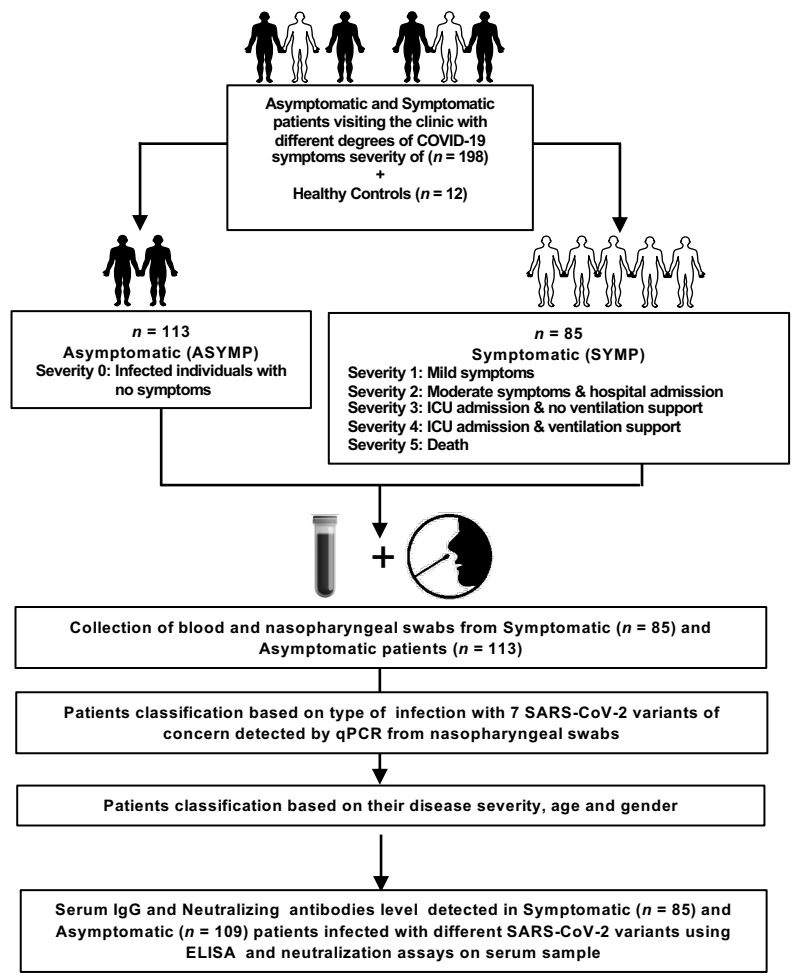
747 The first-generation Spike-alone-based COVID-19 vaccines have successfully reduced the risk of
748 hospitalization, serious illness, and death caused by SARS-CoV-2 infections (1-3, 11, 12). However,
749 waning immunity induced by these vaccines failed to prevent immune escape by many VOCs that have
750 emerged from 2020 to 2024, resulting in a prolonged COVID-19 pandemic.

751

752

753

Fig. 1 Zayou et al.



Variants of Concern	Nonsynonymous Mutation						Total Sample Size (%)
	Δ 69-70	242-244	N501Y	E484K	L452R	T478K	
B.1.1.7 (Alpha)	Positive	Negative	Positive	Negative	Negative	Negative	22 (11.1)
B.1.351(Beta)	Negative	Positive	Positive	Positive	Negative	Negative	17 (8.6)
P.1. (Gamma)	Negative	Negative	Positive	Positive	Negative	Negative	19 (9.6)
B.1.617.2 (Delta)	Negative	Negative	Negative	Negative	Positive	Positive	44 (22.2)
B.1.427/B.1.429 (Epsilon)	Negative	Negative	Negative	Negative	Positive	Negative	31 (15.7)
B.1.1.529 (BA.1) Omicron	Positive	Negative	Positive	Positive	Negative	Positive	35 (17.7)
B.1.1.529 (BA.2) Omicron	Negative	Negative	Positive	Positive	Negative	Positive	30 (15.1)

Table 2. Zayou et al.

Variants of Concern	Symptom		Gender		Age		Total Sample Size (%)
	SYMP (%)	ASYMP (%)	Male (%)	Female (%)	Young (%)	Old (%)	
B.1.1.7 (Alpha)	10 (45.4)	12 (54.6)	12 (54.5)	10 (45.5)	14 (63.6)	8 (36.4)	22 (11.1)
B.1.351(Beta)	8 (47.1)	9 (52.9)	8 (47.1)	9 (52.9)	11 (64.7)	6 (35.3)	17 (8.6)
P.1. (Gamma)	6 (31.5)	13 (68.5)	9 (47.3)	10 (52.7)	10 (52.7)	9 (47.3)	19 (9.6)
B.1.617.2 (Delta)	18 (40.9)	26 (59.1)	24 (54.5)	20 (45.5)	24 (54.5)	20 (45.5)	44 (22.2)
B.1.427/B.1.429 (Epsilon)	16 (51.6)	15 (48.4)	17 (54.8)	14 (45.2)	20 (64.5)	11 (35.5)	31 (15.7)
B.1.1.529 (BA.1) Omicron	17 (48.5)	18 (51.5)	16 (45.7)	19 (54.3)	16 (45.7)	19 (54.3)	35 (17.7)
B.1.1.529 (BA.2) Omicron	10 (33.3)	20 (66.7)	16 (53.3)	14 (46.7)	16 (53.3)	14 (46.6)	30 (15.1)

Fig. 2 Zayou et al.

Conserved Epitopes

S585-588

h-CoV-2/Wuhan (MN908947.3)	Q F G R D I A D T T D A V R D P Q T L E I L D I T P C S F G G V S V I
h-CoV-2/WA/USA2020 (IQ294668.1)	Q F G R D I A D T T D A V R D P Q T L E I L D I T P C S F G G V S V I
h-Cov-2/Alpha (B.1.1.7) (OL689449-1)	Q F G R D I A D T T D A V R D P Q T L E I L D I T P C S F G G V S V I
h-CoV-2/Beta (B.1.351) (MZ314,38)	Q F G R D I A D T T D A V R D P Q T L E I L D I T P C S F G G V S V I
h-CoV-2/Gamma (P.1) (MZ427312.1)	Q F G R D I A D T T D A V R D P Q T L E I L D I T P C S F G G V S V I
h-CoV-2/Delta (B.1.617.2) (OK091006.1)	Q F G R D I A D T T D A V R D P Q T L E I L D I T P C S F G G V S V I
h-CoV-2/Omicron (B.1.1.529) (OM570283.1)	Q F G R D I A D T T D A V R D P Q T L E I L D I T P C S F G G V S V I

S1139-1160

h-CoV-2/Wuhan (MN908947.3)	V N N T V Y D P L Q P E L D S F K E E L D K Y F K N H T
h-CoV-2/WA/USA2020 (IQ294668.1)	V N N T V Y D P L Q P E L D S F K E E L D K Y F K N H T
h-Cov-2/Alpha (B.1.1.7) (OL689449-1)	V N N T V Y D P L Q P E L D S F K E E L D K Y F K N H T
h-CoV-2/Beta (B.1.351) (MZ314,38)	V N N T V Y D P L Q P E L D S F K E E L D K Y F K N H T
h-CoV-2/Gamma (P.1) (MZ427312.1)	V N N T V Y D P L Q P E L D S F K E E L D K Y F K N H T
h-CoV-2/Delta (B.1.617.2) (OK091006.1)	V N N T V Y D P L Q P E L D S F K E E L D K Y F K N H T
h-CoV-2/Omicron (B.1.1.529) (OM570283.1)	

S889-900

h-CoV-2/Wuhan (MN908947.3)	F G A G A A L Q I P F A M Q M A Y R F N G I
h-CoV-2/WA/USA2020 (IQ294668.1)	F G A G A A L Q I P F A M Q M A Y R F N G I
h-Cov-2/Alpha (B.1.1.7) (OL689449-1)	F G A G A A L Q I P F A M Q M A Y R F N G I
h-CoV-2/Beta (B.1.351) (MZ314,38)	F G A G A A L Q I P F A M Q M A Y R F N G I
h-CoV-2/Gamma (P.1) (MZ427312.1)	F G A G A A L Q I P F A M Q M A Y R F N G I
h-CoV-2/Delta (B.1.617.2) (OK091006.1)	
h-CoV-2/Omicron (B.1.1.529) (OM570283.1)	

S153-171

h-CoV-2/Wuhan (MN908947.3)	S Q C V N L T T R T Q L P P A Y T N S F T R G V Y
h-CoV-2/WA/USA2020 (IQ294668.1)	S Q C V N L T T R T Q S Y T N S F T R G V Y
h-Cov-2/Alpha (B.1.1.7) (OL689449-1)	S Q C V N L T T R T Q L P P A Y T N S F T R G V Y
h-CoV-2/Beta (B.1.351) (MZ314,38)	S Q C V N L T T R T Q L P P A Y T N S F T R G V Y
h-CoV-2/Gamma (P.1) (MZ427312.1)	S Q C V N L T T R T Q L P P A Y T N S F T R G V Y
h-CoV-2/Delta (B.1.617.2) (OK091006.1)	S Q C V N L T T R T Q L P P A Y T N S F T R G V Y
h-CoV-2/Omicron (B.1.1.529) (OM570283.1)	S Q C V N L T T R T Q S Y T N S F T R G V Y

S558-565

h-CoV-2/Wuhan (MN908947.3)	F R K S N L K P F E R D I S T E I Y Q A G S T P C N G V E G
h-CoV-2/WA/USA2020 (IQ294668.1)	F R K S N L K P F E R D I S T E I Y Q A G S T P C N G V E G
h-Cov-2/Alpha (B.1.1.7) (OL689449-1)	F R K S N L K P F E R D I S T E I Y Q A G S T P C N G V E G
h-CoV-2/Beta (B.1.351) (MZ314,38)	F R K S N L K P F E R D I S T E I Y Q A G S T P C N G V K G
h-CoV-2/Gamma (P.1) (MZ427312.1)	F R K S N L K P F E R D I S T E I Y Q A G S T P C N G V K G
h-CoV-2/Delta (B.1.617.2) (OK091006.1)	
h-CoV-2/Omicron (B.1.1.529) (OM570283.1)	

S544-570

h-CoV-2/Wuhan (MN908947.3)	N G L T G T G V L T E S N K K F L P F Q Q F G R D I A D T T D A V R D
h-CoV-2/WA/USA2020 (IQ294668.1)	N G L T G T G V L T E S N K K F L P F Q Q F G R D I D D T T D A V R D
h-Cov-2/Alpha (B.1.1.7) (OL689449-1)	N G L T G T G V L T E S N K K F L P F Q Q F G R D I A D T T D A V R D
h-CoV-2/Beta (B.1.351) (MZ314,38)	N G L T G T G V L T E S N K K F L P F Q Q F G R D I A D T T D A V R D
h-CoV-2/Gamma (P.1) (MZ427312.1)	N G L T G T G V L T E S N K K F L P F Q Q F G R D I A D T T D A V R D
h-CoV-2/Delta (B.1.617.2) (OK091006.1)	
h-CoV-2/Omicron (B.1.1.529) (OM570283.1)	

S585-588

h-CoV-2/Wuhan (MN908947.3)	D A V D C A L D P L S E T K C T L K S F T V E K G I Y Q T S N
h-CoV-2/WA/USA2020 (IQ294668.1)	D A V D C A L D P L S E T K C T L K S F T V E K G I Y Q T S N
h-Cov-2/Alpha (B.1.1.7) (OL689449-1)	D A V D C A L D P L S E T K C T L K S F T V E K G I Y Q T S N
h-CoV-2/Beta (B.1.351) (MZ314,38)	D A V D C A L D P L S E T K C T L K S F T V E K G I Y Q T S N
h-CoV-2/Gamma (P.1) (MZ427312.1)	D A V D C A L D P L S E T K C T L K S F T V E K G I Y Q T S N
h-CoV-2/Delta (B.1.617.2) (OK091006.1)	D A V D C A L D P L S E T K C T L K S F T V E K G I Y Q T S N
h-CoV-2/Omicron (B.1.1.529) (OM570283.1)	D A V D C A L D P L S E T K C T L K S F T V E K G I Y Q T S N

S585-588

h-CoV-2/Wuhan (MN908947.3)	F P N I T N L C P F G E V F N A T R F A S V Y A W N R K
h-CoV-2/WA/USA2020 (IQ294668.1)	F P N I T N L C P F G E V F N A T R F A S V Y A W N R K
h-Cov-2/Alpha (B.1.1.7) (OL689449-1)	F P N I T N L C P F G E V F N A T R F A S V Y A W N R K
h-CoV-2/Beta (B.1.351) (MZ314,38)	F P N I T N L C P F G E V F N A T R F A S V Y A W N R K
h-CoV-2/Gamma (P.1) (MZ427312.1)	F P N I T N L C P F G E V F N A T R F A S V Y A W N R K
h-CoV-2/Delta (B.1.617.2) (OK091006.1)	
h-CoV-2/Omicron (B.1.1.529) (OM570283.1)	

S1145-1172

h-CoV-2/Wuhan (MN908947.3)	L D S F K E E L D K Y F K N H T S P D V D L G D I S G I
h-CoV-2/WA/USA2020 (IQ294668.1)	L D S F K E E L D K Y F K N H T S P D V D L G D I S G I
h-Cov-2/Alpha (B.1.1.7) (OL689449-1)	L D S F K E E L D K Y F K N H T S P D V D L G D I S G I
h-CoV-2/Beta (B.1.351) (MZ314,38)	L D S F K E E L D K Y F K N H T S P D V D L G D I S G I
h-CoV-2/Gamma (P.1) (MZ427312.1)	L D S F K E E L D K Y F K N H T S P D V D L G D I S G I
h-CoV-2/Delta (B.1.617.2) (OK091006.1)	
h-CoV-2/Omicron (B.1.1.529) (OM570283.1)	

S411-501

h-CoV-2/Wuhan (MN908947.3)	E I Y Q A G S T P C N G V E G F N C Y F P L Q S Y G F Q P T N
h-CoV-2/WA/USA2020 (IQ294668.1)	E I Y Q A G N K P C N G V A G V N C Y F P L Q S Y G F R P T Y
h-Cov-2/Alpha (B.1.1.7) (OL689449-1)	E I Y Q A G S T P C N G V E G F N C Y F P L Q S Y G F Q P T Y
h-CoV-2/Beta (B.1.351) (MZ314,38)	E I Y Q A G S T P C N G V K G F N C Y F P L Q S Y G F Q P T Y
h-CoV-2/Gamma (P.1) (MZ427312.1)	E I Y Q A G S T P C N G V K G F N C Y F P L Q S Y G F Q P T Y
h-CoV-2/Delta (B.1.617.2) (OK091006.1)	E I Y Q A G S K P C N G V E G F N C Y F P L Q S Y G F Q P T N
h-CoV-2/Omicron (B.1.1.529) (OM570283.1)	E I Y Q A G N K P C N G V A G F N C Y F P L R S Y G F R P T Y

S538-563

h-CoV-2/Wuhan (MN908947.3)	F G E V F N A T R F A S V Y A W N R K R I S N C V A
h-CoV-2/WA/USA2020 (IQ294668.1)	F D E V F N A T T F A S V Y A W N R K R I S N C V A
h-Cov-2/Alpha (B.1.1.7) (OL689449-1)	F G E V F N A T R F A S V Y A W N R K R I S N C V A
h-CoV-2/Beta (B.1.351) (MZ314,38)	F G E V F N A T R F A S V Y A W N R K R I S N C V A
h-CoV-2/Gamma (P.1) (MZ427312.1)	F G E V F N A T R F A S V Y A W N R K R I S N C V A
h-CoV-2/Delta (B.1.617.2) (OK091006.1)	F G E V F N A T R F A S V Y A W N R K R I S N C V A
h-CoV-2/Omicron (B.1.1.529) (OM570283.1)	F D E V F N A T R F A S V Y A W N R K R I S N C V A

S589-593

h-CoV-2/Wuhan (MN908947.3)	Y N S A S F S T F K C Y G V S P T K L N D L C F T
h-CoV-2/WA/USA2020 (IQ294668.1)	Y N F A P F F A F K C Y G V S P T K L N D L C F T
h-Cov-2/Alpha (B.1.1.7) (OL689449-1)	Y N S A S F S T F K C Y G V S P T K L N D L C F T
h-CoV-2/Beta (B.1.351) (MZ314,38)	Y N S A S F S T F K C Y G V S P T K L N D L C F T
h-CoV-2/Gamma (P.1) (MZ427312.1)	Y N S A S F S T F K C Y G V S P T K L N D L C F T
h-CoV-2/Delta (B.1.617.2) (OK091006.1)	Y N S A S F S T F K C Y G V S P T K L N D L C F T
h-CoV-2/Omicron (B.1.1.529) (OM570283.1)	Y N X A P F F A F K C Y G V S P T K L N D L C F T

S585-588

h-CoV-2/Wuhan (MN908947.3)	V C G P K K S T N L V K N K C V N F N F N G L T G T G V L T E S N K K
h-CoV-2/WA/USA2020 (IQ294668.1)	V C G P K K S T N L V K N K C V N F N F N G L T G T G V L T E S N K K
h-Cov-2/Alpha (B.1.1.7) (OL689449-1)	V C G P K K S T N L V K N K C V N F N F N G L T G T G V L T E S N K K
h-CoV-2/Beta (B.1.351) (MZ314,38)	V C G P K K S T N L V K N K C V N F N F N G L T G T G V L T E S N K K
h-CoV-2/Gamma (P.1) (MZ427312.1)	V C G P K K S T N L V K N K C V N F N F N G L T G T G V L T E S N K K
h-CoV-2/Delta (B.1.617.2) (OK091006.1)	V C G P K K S T N L V K N K C V N F N F N G L T G T G V L T E S N K K
h-CoV-2/Omicron (B.1.1.529) (OM570283.1)	V C G P K K S T N L V K N K C V N F N F N G L T G T G V L T E S N K K

S146-170

h-CoV-2/Wuhan (MN908947.3)	N L D S K V G G N N Y L Y R L F R K S N L K P F E R D I S T
h-CoV-2/WA/USA2020 (IQ294668.1)	N L D S K V G G N N Y L Y R L F R K S N L K P F E R D I S T
h-Cov-2/Alpha (B.1.1.7) (OL689449-1)	N L D S K V G G N N Y L Y R L F R K S N L K P F E R D I S T
h-CoV-2/Beta (B.1.351) (MZ314,38)	N L D S K V G G N N Y L Y R L F R K S N L K P F E R D I S T
h-CoV-2/Gamma (P.1) (MZ427312.1)	N L D S K V G G N N Y L Y R L F R K S N L K P F E R D I S T
h-CoV-2/Delta (B.1.617.2) (OK091006.1)	
h-CoV-2/Omicron (B.1.1.529) (OM570283.1)	

S889-900

h-CoV-2/Wuhan (MN908947.3)	F S Q I L P D P S K P S K R S F I E
h-CoV-2/WA/USA2020 (IQ294668.1)	F S Q I L P D P S K P S K R S F I E
h-Cov-2/Alpha (B.1.1.7) (OL689449-1)	F S Q I L P D P S K P S K R S F I E
h-CoV-2/Beta (B.1.351) (MZ314,38)	F S Q I L P D P S K P S K R S F I E
h-CoV-2/Gamma (P.1) (MZ427312.1)	F S Q I L P D P S K P S K R S F I E
h-CoV-2/Delta (B.1.617.2) (OK091006.1)	
h-CoV-2/Omicron (B.1.1.529) (OM570283.1)	

S601-608

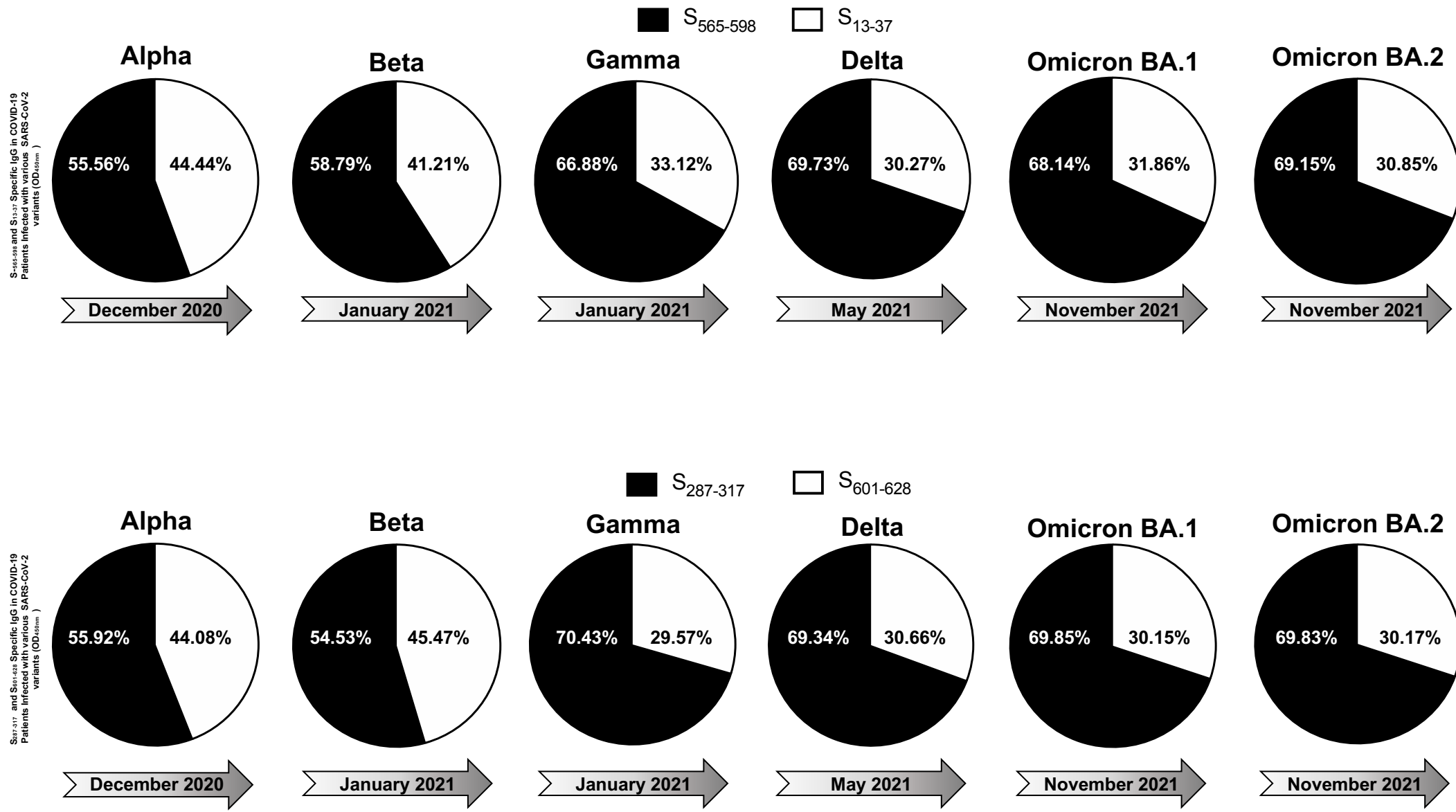
h-CoV-2/Wuhan (MN908947.3)	G T N T S N Q V A V L Y Q D V N C T E V P V A I H A D Q
h-CoV-2/WA/USA2020 (IQ294668.1)	G T N T S N Q V A V L Y Q G V N C T E V P V A I H A D Q
h-Cov-2/Alpha (B.1.1.7) (OL689449-1)	G T N T S N Q V A V L Y Q G V N C T E V P V A I H A D Q
h-CoV-2/Beta (B.1.351) (MZ314,38)	G T N T S N Q V A V L Y Q G V N C T E V P V A I H A D Q
h-CoV-2/Gamma (P.1) (MZ427312.1)	G T N T S N Q V A V L Y Q G V N C T E V P V A I H A D Q
h-CoV-2/Delta (B.1.617.2) (OK091006.1)	G T N T S N Q V A V L Y Q G V N C T E V P V A I H A D Q
h-CoV-2/Omicron (B.1.1.529) (OM570283.1)	G T N T S N Q V A V L Y Q G V N C T E V P V A I H A D Q

S514-500

h-CoV-2/Wuhan (MN908947.3)	Q D V N C T E V P V A I H A D Q L T P T W R V Y S T G S
h-CoV-2/WA/USA2020 (IQ294668.1)	G D V N C T E V P V A I H A D Q L T P T W R V Y S T G S
h-Cov-2/Alpha (B.1.1.7) (OL689449-1)	G D V N C T E V P V A I H A D Q L T P T W R V Y S T G S
h-CoV-2/Beta (B.1.351) (MZ314,38)	G D V N C T E V P V A I H A D Q L T P T W R V Y S T G S
h-CoV-2/Gamma (P.1) (MZ427312.1)	G D V N C T E V P V A I H A D Q L T P T W R V Y S T G S
h-CoV-2/Delta (B.1.617.2) (OK091006.1)	G D V N C T E V P V A I H A D Q L T P T W R V Y S T G S
h-CoV-2/Omicron (B.1.1.529) (OM570283.1)	G D V N C T E V P V A I H A D Q L T P T W R V Y S T G S

Non-Conserved Epitopes

Fig. 3 Zayou et al.



S₂₈₇₋₃₁₇

